AN INNOVATIVE ISOLATION BEARING
WITH SHAPE MEMORY ALLOYS

G. Attanasi[1], F. Auricchio[2], C. Crosti[3] and G. L. Fenves[4]

[1] *PhD Student , European School for Advanced Studies in Reduction of Seismic Risk,
ROSE School, Pavia, Italy*

[2] *Professor, Department of Structural Mechanics, Università degli Studi di Pavia, Italy*

[3]*Agom International spa, Ossona, Milano, Italy*

[4] *Professor, Department of Civil and Environmental Engineering, University of California, Berkeley*

Email: gattanasi@roseschool.it, auricchio@unipv.it, fenves@berkeley.edu

ABSTRACT :

This paper presents a new isolation device concept using shape memory alloy elements, to evaluate the possibility of its application and to investigate the effectiveness in reaching the structural design goals compared with traditional isolation devices. Shape memory alloys (SMAs) are characterized by unique mechanical properties due to solid-solid transformation between phases of the alloy. The nonlinear hysteresis due to the superelastic effect, which can be described by a flag shape relation, provides supplemental damping, reduction on the residual deformation given by the recover of the original shape, and limitation on the force transmitted to the connected elements. Moreover it is possible to obtain high strength and strain capacity, high resistance to corrosion and to fatigue. Actual devices used in base isolated systems have been taken into account and "equivalent" SMA isolation devices have been designed to get the same characteristics in term of global structure period elongation, displacement capacity, capability to sustain the base shear and the vertical load, but also in order to provide energy dissipation and to sensibly reduce residual deformations. The design device process has been then checked through numerical analyses comparing the response of SMA bearing systems and "traditional" bearing systems and their effectiveness on the global structural response.

KEYWORDS: seismic isolation, shape memory alloys, superelastic effect.

1. INTRODUCTION TO SEISMIC ISOLATION

Seismic isolation is a technology which mitigates the earthquake effects on buildings and their potentially vulnerable contents. The concept of protecting a structure from the damaging effects of an earthquake introducing a support isolating the building from the shaking ground is quite old, but research continues for effective, economical, and reliable seismic isolation systems. Advantages in seismic isolation are evident: first, the level of damage is more safely controlled and confined to generally well-replaceable spots; then, an isolation system not only damps and reduces the action demand of the global structure, but also limits the force transmittable to the superstructure. However, design of isolated structures has some particular concerns. Practical isolation systems must balance between the extent of force limitation and acceptable relative displacements across the isolation system during earthquakes. For this purpose, additional damping can be useful, because both forces transmitted and deformations within the structure are reduced. In general, seismic design of the superstructure will be considerably simplified, apart from the service connections need to accommodate the large displacements across the isolating layer.

1.1 Fundamental Concepts
Seismic isolation is a technique for reducing the seismic risk in different types of structures modifying the global response and improving the structural performance. The objective is to regularize the response and to modify the relative effective stiffness and strength in the structure. In fact, isolation layer is more flexible with

respect to the rest of the structure, hence it absorbs a large part of the displacement demand. Since the displacement demand of the superstructure is small, we can assure its elastic response. Moreover, if we use nonlinear isolation system devices, the maximum base shear transmitted to the superstructure is limited and capacity design can be performed. In this way all the nonlinear and dissipating phenomena occur at the isolation level avoiding any brittle failure mode.

Fundamental period of the isolated structure increases with respect the one in the not isolated condition, inferring to either the displacement or the acceleration demand. Moreover the isolated fundamental mode is characterized by a large participating mass, almost equal to the total mass. Therefore the isolation system determines the first period and damping of an isolated structure, and these, in their turn, control the structure seismic response.

The presence of isolation system can even increase the global energy dissipation capacity of the structure and this helps to reduce the displacement demand.

2. SHAPE MEMORY ALLOYS

Shape memory alloy (SMA) is a novel functional material with increasing applications in many areas, recently also in response control of civil structures.

2.1 Basics on Shape Memory Alloys
The first record of the shape memory transformation was the observation of a reversible phase transformation in the gold-cadmium (AuCd), but the shape memory effect was discovered in the nickel-titanium (the material was named Nitinol). Among the various alloys, nickel-titanium, also called Nitinol, possesses superior thermo-mechanical and thermo-electrical properties and is the most commonly used SMA. In this work, SMAs are referred to as Nitinol SMAs.

2.1.1 Shape Memory and Superelastic Effects
The most important properties showed by the SMA are the shape memory and the superelastic effects. These are the result of reversible phase transformations of SMAs. There are two crystal structure phases in SMAs: the austenite one, stable in high temperature, and the martensite one, stable in low temperature. In its low temperature phase, SMAs exhibit the shape memory effect (SME). When SMAs in martensite are subjected to external stress, they deform through a so-called detwining mechanism. From its martensitic form, the SMAs are easily deformed to several percent strain. Unloading results in a residual strain, as shown in (Fig.1a). In its high temperature form, SMAs exhibit a superelastic effect. Originally in austenitic phase, martensite is formed upon loading beyond a certain stress level, resulting in the stress plateau shown in (Fig.1b). However, upon unloading, the martensite becomes unstable, resulting in a transformation back to austenite and the recovery of the original, undeformed shape.

2.1.2 Other Mechanical Properties of Shape Memory Alloys
Regarding the cyclic behavior of SMA, repeated cyclical loading leads to gradual increases in the residual strains. This results from the occurrence of micro-structural slips during the stress-induced martensitic transformation, which causes residual strains and internal stresses. The other observation is that the forward transformation stress decreases for increasing number of cycle.

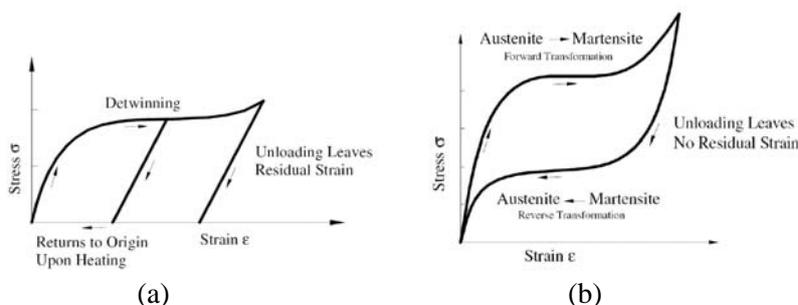(a)   (b)
Figure 1: idealized stress-strain curve for shape memory effect (a) and for superelastic effect (b)
[from (Desroches and Smith 2003)].

However, the reduction in the reverse transformation is less than that in the forward phase transformation. The degradation of the cyclical properties of the SMAs, known as fatigue, can be improved. In fact training, which consists of pre-cycling of the specimen, decreases the fatigue effect.

Concerning temperature, it is likely the single most important factor when predicting the behavior of shape memory alloys. The shape memory process is a thermo-elastic process, meaning that a decrease in temperature is equivalent to an increase in stress. Therefore, as the temperature decreases, an increase in stress results, thereby a lower stress value is required to induce transformation.

3. FEASIBILITY OF SMA TECHNOLOGY FOR SEISMIC ISOLATION APPLICATION

In this context, the definition "shape memory alloys device" refers to a bearing systems characterized by a non-linear horizontal force-displacement relation which can be described by a flag-shape hysteresis, as shown in Fig.2.
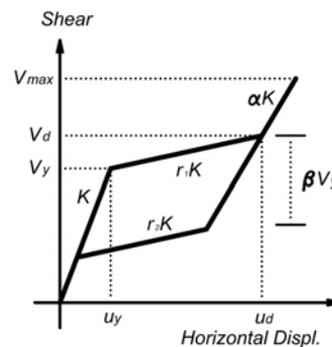

Figure 2: parameters for the SMA superelastic force-displacement model.

The key parameters characterizing the nonlinear behavior of the device Fig.2 are:
   o *K, r$_1$K, r$_2$K, αK* are respectively the initial stiffness, the second stiffness in loading and the second stiffness in unloading and the second hardening stiffness;
   o *V$_d$*, *u$_d$*, *V$_y$*, *u$_y$* are respectively the design shear and displacement and the yielding shear and displacement of the device, while *V$_{max}$* is the maximum lateral force which the device can stand without breaking;
   o *β V$_y$* is the lateral force difference between the level of force at which the first transformation (when it is loaded) occurs and the level of force at which the second transformation (when it is unloaded) occurs; therefore *β* is a parameter that measure the dissipation capability of the flag-shape hysteresis.

The device we consider behaves in the same way both in tension and in compression, which implies the force-displacement relation is symmetric respect the origin between first and third quadrant.

3.1 SMA Technology Isolation Device Design
To evaluate the advisability in using a SMA technology in base isolation we assume to be able to design and manufacture a SMA bearing based on the superelastic effect for the horizontal force-displacement relation. At this first stage of work, since we are still investigating the feasibility of the concept, the device has been defined just in terms of hysteresis rule.

Table 1: nominal design properties of reference lead rubber bearing diameter 500 mm (a) and elastoplastic model parameters (b) [courtesy AGOM International srl].

LRB 500	
diameter	500 mm
effective horizontal stiffness	1.62 kN/mm
seismic comb. vertical load	1653 kN
seismic design displacement	162 mm
hysteretic damping ratio	28%

(a)

LRB 500		
yielding shear	V_y	147 kN
design shear	V_d	262 kN
yielding displacement	u_y	17.5 mm
design displacement	u_d	162 mm
initial stiffness	k	8.4 kN/mm
second stiffness	rk	0.8 kN/mm

(b)

3.1.1 Goal of the Design Process
We model a SMA bearing device with equivalent properties of an actual nonlinear isolator. Obviously the SMA device is characterized by a different force-displacement relation, but it has the same yielding and design forces, and the same yielding and design displacements with respect to a traditional device. Therefore in this context, the concept of equivalence involves that the two different nonlinear relations are characterized by the same initial and second stiffness and the same yielding force and strength. This choice affects the secant stiffness computation according the Direct Displacement Based Design approach design philosophy (Priestley et al. 2007). Hence given that the effective periods are the same and from a DDBD point of view the only difference between the traditional bearing and the actual isolation device is the nominal hysteretic energy dissipation.

3.1.2 Reference Isolator Device
The isolator we consider as a starting point for the referring parameters is an actual lead rubber bearing, which has been fully characterized by an experimental campaign. It is produced by *AGOM International srl* and the nominal parameters used for the design purpose are listed in Tab.1.
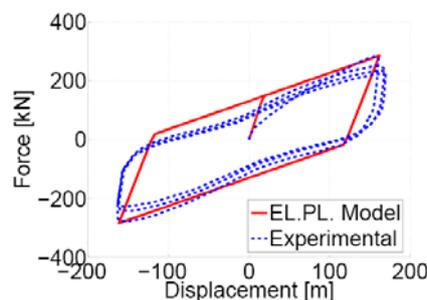

Figure 3: force-deformation relations for LRB 500: comparison of experimental test and elastoplastic model (experimental data and model parameters have been provided by *AGOM International srl*).

Results of experimental tests carried on the bearings are shown in Fig.3, compared with the elasto-plastic hysteresis used to model it. Elastoplastic model is clearly an approximation of the real behavior of the isolator. In particular, the comparison with the experimental results shows that the elastoplastic model does not estimate the initial stiffness nor the degradation well. However, for the representation of the general characteristics of the devices, the adopted model is acceptable, being exact in terms of secant stiffness at the design displacement and giving a good estimation, even if not exact, of the hysteretic energy dissipated and of residual displacements.

3.1.3 Equivalent SMA Isolator Device
We simulate the idealized design of an equivalent SMA isolator considering the properties of the lead rubber bearing. Starting from the elastoplastic model of the actual device as described in Tab.1 we use an equivalent flag-shape model referring to the hysteresis in Fig.2. Consistently with the latest, we describe SMA device force-displacement relation using parameters summarized in Tab.2.

Table 2: flag-shape model parameters for SMA bearing equivalent to LRB diameter 500 mm [parameters as shown in Fig.2].

SMA eq. LRB500		
yielding shear	V_y	**147 kN**
design shear	V_d	**262 kN**
yielding displacement	u_y	**17.5 mm**
design displacement	u_d	**162 mm**
initial stiffness	k	**8.4 kN/mm**
second stiffness	rk	**0.8 kN/mm**

With respect to model in Fig.2 we consider $r_1 = r_2 = r$, which means that the device has the same stiffness for loading and unloading in the flag-shape plateau, and we assume a large ductility available in the flag-plateau, so that the final hardening occurs far away from the area of displacement we care about. Finally, we take into account a large dissipation capability of the flag-shape hysteresis, considering *β = 95%*.

3.2 Flag-Shape Hysteresis Reduction Factor Estimation Using the Equivalent Damping Approach

The equivalent damping modeling and estimation, given by the contribution of the elastic and hysteretic component is a key point in the isolation devices design because it strongly affects the structural displacement demand. Moreover in our analysis and comparison, we consider two systems with the same secant stiffness, because the design displacement and shear are the same, and initial and second stiffness are also the same: therefore according a displacement based approach the most important difference is given by the damping ratio. As shown in Fig.4, we compare two very different relations. Following the area-based Jacobsen approach (Grant et al. 2005) to determine the equivalent hysteretic damping estimation we would get, as a function of the ductility μ and for a maximum flag-shape dissipation capability ($\beta = 100\%$), the relation for hysteretic damping component and for force and displacement reduction factor as shown in Fig.5.
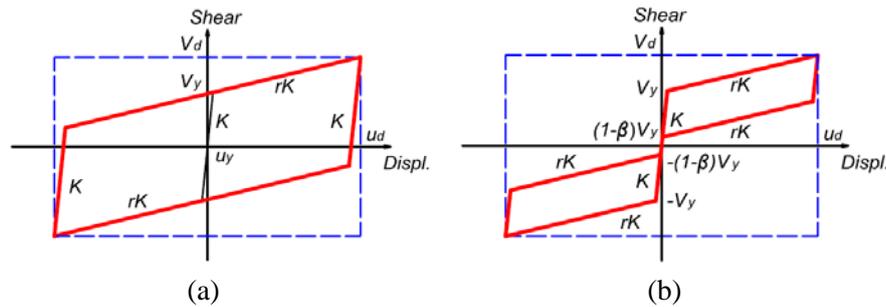

(a)   (b)

Figure 4: hysteretic area-based analysis comparison for elasto-plastic model (a) and flag-shape model (b).

The area-based approach for hysteretic damping estimation leads to the conclusion that an isolation device based on a SMA technology and flag-shape hysteresis is always supposed to be significantly less favorable in terms of displacement and force demand respect to a similar system based on elastoplastic hysteresis. This is because the damping reduction factor computed considering the hysteresis results to be significantly lower for SMA flag shape force displacement relation respect to LRB elastoplastic relation. Nevertheless, we do not have evidences of the suitability of the approach itself to determine the hysteretic energy dissipation for flag-shape force-displacement relation with high ductility demand.
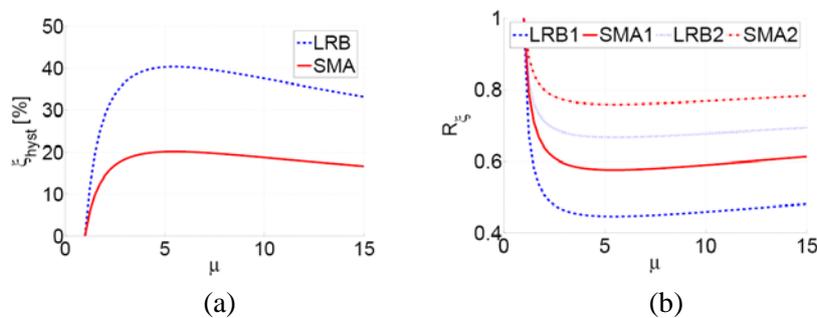

(a)   (b)

Figure 5: hysteretic area-based damping comparison as a function of ductility (a) and force and displacement reduction factor computed for far field and near field events (b)

3.3 Effective Seismic Response Evaluation of Different Hysteresis Isolation Devices

To investigate the response of a shape memory alloy isolator device and to compare it with the response of an equivalent classical lead rubber bearing, we perform time history analyses.

Given an isolated structure, which has been designed considering a simulated project consistent with the properties of the actual lead rubber bearing, we perform the analysis set considering a rigid superstructure approach, assuming that all the displacement occurs at the isolation system level. The system hence can be modelled as a single degree of freedom system in which the superstructure is participating only as an additional mass.

We repeat the analysis three times, modelling the isolation system taking into account:
- elasto-plastic model (Fig.6a). It is representative of the real lead rubber bearing device and the parameters we use are those reported in Tab.1a;

- flag-shape model (Fig.6b). It reproduces the shear-horizontal displacement relation of the shape memory alloy device characterized by the design properties reported in Tab.2. We target a device that performs like the real LRB system in the sense of equivalent shear and displacement capacity and initial and second stiffness;
- linear elastic model (Fig.6c). Given the design displacement u_d and the design shear V_d, common for the previous models, we consider the equivalent linear system, using parameters reported in Tab.1b.

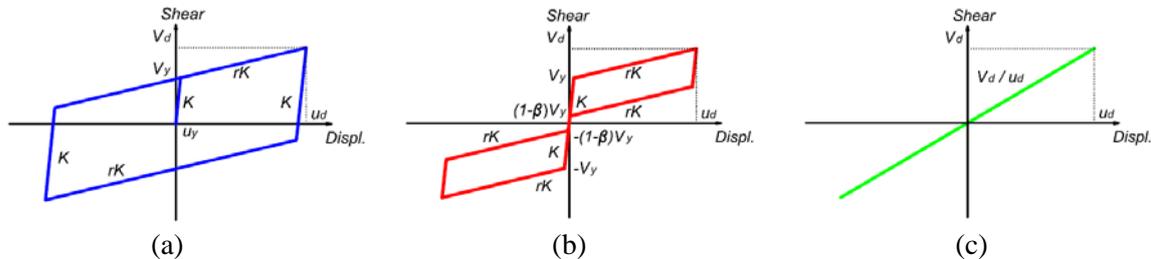|		
(a)	(b)	(c)

Figure 6: base shear horizontal displacement model for lead rubber bearing (a),
shape memory alloy (b) and equivalent linear elastic with secant stiffness (c) isolation device.

We model the elastic damping component considering a *5%* elastic damping in the equivalent secant stiffness. Regarding the nonlinear models, we consider a constant damping ratio (proportional to the initial stiffness) in order to have the same damping energy with respect the previous one if the displacement history is the same. It turns out that given the different critical damping, to have the same nominal dissipation capability the damping ratio in elastoplastic and flag-shape model the damping ratio has to be equal to *2.2%*. The reason of having the same elastic dissipation capability is to be consistent in result comparison and get an estimation of the hysteretic effect in terms of energy balance, displacement and force demand reduction.

We used seven scaled natural ground motions for the analysis compatible with Eurocode 8 spectra *Pga = 0.25g* and soil *C*, 5% elastic damping ratio type *1*. They are listed in Tab.3.

Table 3: ground motion records considered in the analysis

Earthquake	Date	Location	Comp.	PGA [g]	PGV [m/s]	PGD [m]	Scaling factor	PGA [g]	PGV [m/s]	PGD [m]
Tabas	16 Sep 78	Tabas stat.	FN	0.900	1.100	0.513	0.6257	0.563	0.689	0.321
Tabas	16 Sep 78	Tabas stat.	FP	0.977	1.058	0.752	0.6382	0.624	0.675	0.480
Erzinican	13 Mar 92	Meteor. stat.	FN	0.432	1.192	0.423	0.6672	0.288	0.795	0.282
Erzinican	13 Mar 92	Meteor. stat.	FP	0.457	0.581	0.295	1.2406	0.567	0.721	0.365
Landers	28 Giu 92	Lucerne	FN	0.713	1.360	2.298	0.6161	0.439	0.838	1.416
Northridge	17 Jan 94	Olive View	FN	0.732	1.222	0.310	0.5847	0.428	0.714	0.181
Kobe	16 Jan 95	Tato	FP	0.424	0.637	0.233	0.7109	0.302	0.453	0.165

3.4 Time History Analysis Results

We perform comparisons between flag shaped, elastoplastic and linear elastic systems considering force and displacement time-history demand and system energy balance. The base shear and displacement demands are reduced in the elastoplastic and flag shape systems with respect the linear elastic equivalent system (Fig.7a-b). This is an expected result because the linear elastic model reproduces the isolation system without any energy dissipation (Fig.7c).

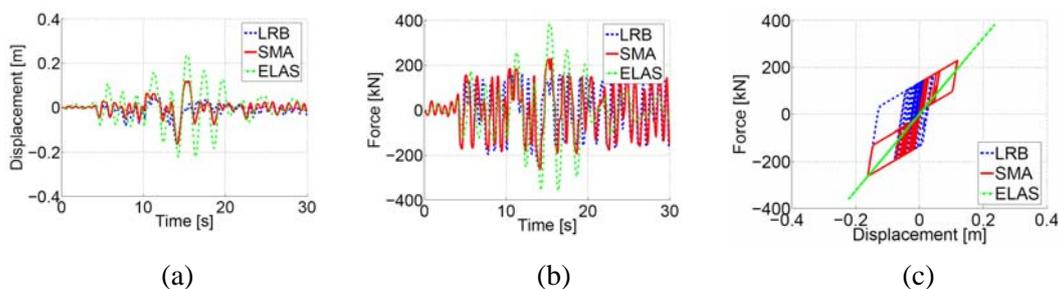|		
(a)	(b)	(c)

Figure 7: comparison between the response of the three models in terms of displacement (a)
and force (b) versus time and force-displacement relation (c) considering Tabas (FP) record.

In particular we are interested in the force and displacement reduction factors, which are the ratio between the demands considering the actual hysteresis force-displacement relation with respect to the one given by a linear elastic secant stiffness model (Fig8a-b); conceptually reduction factor in the analysis conditions represents the effectiveness of the hysteretic energy dissipation. Moreover we evaluate the energy balance of the system in time, looking at the amount of hysteretic dissipated energy over the total input one, as shown in Fig.8c.

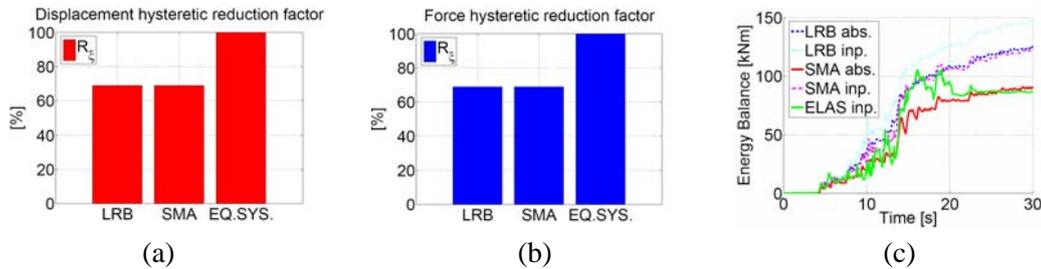(a)   (b)   (c)

Figure 8: maximum displacement (a) and force (b) reduction factor and energy balance comparison (c) between the three systems considering Tabas (FP) record.

General comparison of all the ground motion results in terms of force and displacement reduction factor as well as hysteretic absorbed energy is reported in Fig. 9.

(a)   (b)   (c)
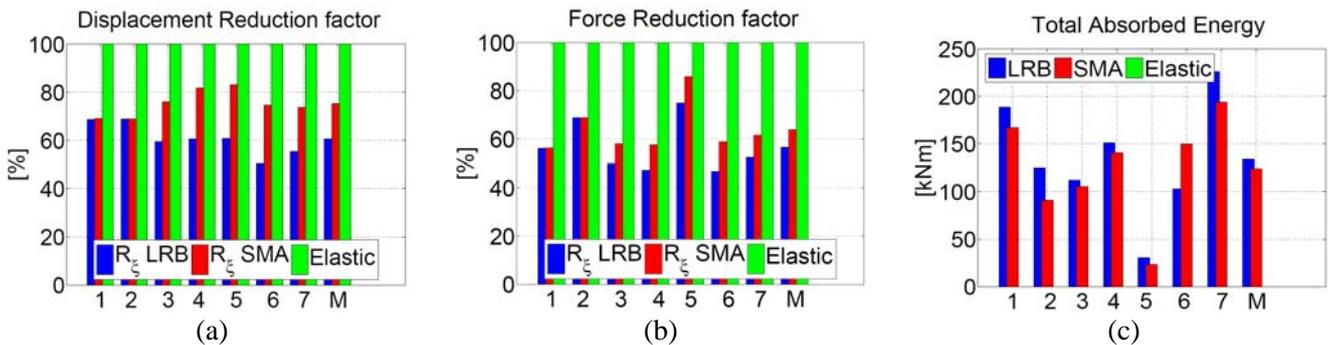
Figure 9: maximum displacement (a) and force (b) reduction factor and absorbed energy (c) comparison between LRB and SMA systems: each set of column corresponds to a ground motion; last set is the mean value.

The first and most important information we can learn from the comparison is that differences between the lead rubber bearing elastoplastic model and shape memory alloy flag shape model are quite small if compared with the linear elastic force and displacement demand. This is shown in Fig.9a-b and proved also by fact that the total absorbed energy, which is the part of input energy dissipated through hysteretic cycles is almost the same between the two nonlinear models. Hence the differences are almost negligible with respect to the fact that the elastoplastic hysteresis is characterized by an area which for the most dissipating case ($\beta = 95\%$) is more than twice of the flag shape one.

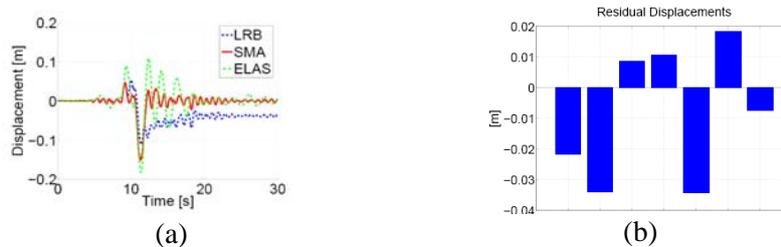(a)   (b)

Figure 10: residual displacement comparison between the three systems in Landers ground motion (a) and residuals in LRB system in all the ground motions (b)

Another issue for isolation bearings is the residual displacement. This is very undesirable in an isolation system device because it leads to the needing of reparation of the system after the seismic event. Of course this problem

strongly affects an elastoplastic model, especially when the seismic input is coming from a near fault event, characterized by a pulse-like load; on the other side, the SMA bearing is supposed to perform zero residual displacements, as shown in Fig.10a, together with all the residual displacement values recorded in the LRB device in all the ground motions (Fig.10b).

4. CONCLUSIONS

An investigation about the feasibility of shape memory alloy technology application to seismic isolation devices has been performed. The evaluation of responses data from time history analyses has been considered the most suitable method to study the problem. We have compared behavior of a model representing a conventional lead rubber bearing device with the behavior of a shape memory technology device and of an equivalent linear elastic model. Results show that the overall behavior of the isolation system characterized by the flag-shape hysteresis is close to the response of isolation system with elastoplastic one. In particular, reduction factors in terms of displacements and forces of LRB and SMA models with respect to linear elastic secant model response are quite similar for large SMA dissipation capability. Also in terms of absorbed energy over input energy ratio differences are small.

Given these results, the conclusion of this investigation is that the SMA application in seismic isolation is possible and can lead to several advantages. SMA devices are characterized by energy dissipation and numerical investigations have demonstrated that it is comparable, for its influence on the response, to the dissipation of actual highly dissipating devices.

Moreover SMA devices have good recentering capability, either because of the superelastic effect, which has been taken into account in this work, or because of the shape memory effect, that can provide a further restoring force if for any reason some residuals are still present.

Possible applications of SMAs in isolating bearing systems are relative to dissipating-recentering additional element for any other bearings, existing or new. Hence in theory we are considering a quite flexible device characterized by large range of application. For instance we can think to apply this kind of restrainer to rubber bearing, in substitution of the lead component, or in friction pendulous system to be able to control not only the horizontal displacement, eventually provide a recentering force if the gravity is not enough to be larger than the friction, but also it could be possible to control a possible uplift.

REFERENCES

Attanasi, G. (2008, April). Feasibility assessment of innovative isolation bearing system with shape memory alloys, Master Thesis, ROSE School, University of Pavia, Italy.

Carr, A. J. (2007). Ruaumoko Manual Volume 4: User Guide to Associated Programs. Department of Civil Engineering, University of Canterbury, ChristChurch, New Zealand.

Christopoulos, C. and A. Filiatrault (2006). Principles of Passive Supplemental Damping and Seismic Isolation. IUSS Press, Pavia.

Desroches, R. and B. Smith (2003). Shape memory alloys in seismic resistant design and retrofit: a critical review of their potential and linitations. Journal of Earthquake Engineering 7, 1–15.

Eurocode 8 (2003). Design of structures for earthquake resistance, part I: General rules, seismic actions and rules for buildings. pre-ENV 1998-1.

Grant, D. N., C. A. Blandon, and M. J. N. Priestley (2005). Modelling Inelastic Response in Direct Displacement Based Design. IUSS Press, Pavia.

Naeim, F. and J. M. Kelly (1999). Desing of Seismic Isolated Structures. From Theory to Practice. John Wiley and Sons, New York.

Priestley, M. J. N., G. M. Calvi, and M. J. Kowalsky (2007). Displacement-Based Seismic Design of Structures. IUSS Press, Pavia.

Skinner, R. I., W. H. Robinson, and G. H. McVerry Isolation. John Wiley and Sons, Chichester.